Journal of Engineering Science and Technology Review 16 (5) (2023) 83 - 90

Research Article

JOURNAL OF
Engineering Science and Technology Review

www.jestr.org

Inspection Path Optimization of the Agricultural Unmanned Aerial Vehicle Based on the Improved PSO Algorithm

Li Li [1,2] and Xuesong Yang [1, *]

[1]*School of Urban Design, Wuhan University, Wuhan 430072, China*
[2]*Teaching Affairs Department, Hubei Engineering University, Xiaogan 432000, China*

Received 11 August 2023; Accepted 15 October 2023

Abstract

A Cauchy-Gaussian particle swarm optimization (PSO) algorithm was proposed to improve the low convergence speed and local optimization problem of unmanned aerial vehicle (UAV) path planning based on the traditional PSO algorithm in the inspection task. The inspection environment of an agricultural UAV was preinspected by a radar sensor, and a flight mission environment model was established. Moreover, adaptive inertia weight and Cauchy-Gaussian mutation operator were introduced to adjust the PSO algorithm, balance the global–local convergence speed, and optimize the local extreme value problem. The track length cost, obstacle collision cost, and elevation cost of the agricultural UAV were comprehensively analyzed, and the fitness function of the agricultural UAV track planning was proposed. Results show that the convergence time of the PSO algorithm optimized by the Cauchy-Gaussian mutation operator is 3.46 s shorter than that of the traditional PSO algorithm. The path length of the PSO algorithm optimized by the Cauchy-Gaussian mutation operator is shorter than that of the traditional PSO algorithm by 12.6735% (6.173 km). The proposed algorithm has stronger robustness and better environmental adaptability than other algorithms. This study provides a good reference for the inspection of agricultural UAVs.

Keywords: Agricultural UAV, Inspection path, PSO algorithm, Adaptive inertia weight, Optimization

1. Introduction

Given the advantages of convenient operation, flexible operation, and real-time accuracy, unmanned aerial vehicles (UAVs) have recently been widely promoted in production and life. Despite their late development in China, UAVs have attracted extensive attention from all walks of life with the rapid development of the economy, science, and technology. Moreover, a series of effective application studies has been conducted. Nowadays, UAVs are widely used in the military field and show high application value in agriculture and forestry development [1]. In general, UAVs can control the spraying equipment through ground remote control or navigation flight control when completing the agricultural tasks of spraying operations and providing strong support for agricultural operations. Agricultural inspection is an important part of modern agriculture development. Introducing UAVs into agricultural inspection can effectively meet the operational requirements of agricultural inspection with high efficiency and low cost [2]. The UAV technology promoted in agricultural inspection is based on network information technology. Based on efficient, convenient, and intelligent research and development, the application value of UAVs in agricultural inspection is significantly enhanced [3]. Given the vast territory of China, the characteristics and planting methods of crops vary in different regions. Moreover, the traditional ground equipment application has certain limitations. The popularization of agricultural inspection UAVs can reduce the workload of farmers and promote the reconstruction of the modern agricultural system, thereby contributing to the mechanization development of agriculture and improving the overall level of agricultural development in China [4].

Agricultural UAVs have several functions. In pest control, agricultural UAVs can accurately spray pesticides on farmland and effectively control the occurrence and spread of pests and diseases [5]. Compared with traditional manual spraying, using UAVs for spraying pesticides allows accurate application and reduces pesticide use and environmental pollution. In fertilization management, agricultural UAVs can achieve precise fertilization, perform fixed-point quantitative fertilization according to the needs of different farmlands, improve crop nutrient utilization efficiency, and increase yield and save costs [6]. Agricultural UAVs are equipped with aerial photography and sensor technology to monitor farmland growth, soil moisture, diseases, and pests in real time. Farmers can know the health status of farmland in time and make reasonable agricultural management decisions through data collection and analysis [7].

2. State of the art

Smart agriculture cloud is an agricultural information platform based on cloud computing technology, which integrates sensors, the Internet of Things, and artificial intelligence into the cloud platform to realize real-time monitoring and management of agricultural production. Smart agriculture cloud platforms can provide analysis, prediction, and decision support for agricultural production data, help farmers master agricultural production, and improve agricultural production efficiency and quality. In agricultural production, monitoring and inspecting crop

*E-mail address: gygy88521@sina.com
ISSN: 1791-2377
doi:10.25103/jestr.165.11

diseases and insect pests often depend on manpower, and the contradiction of insufficient human resources is increasingly prominent. With the continuous development of agricultural aviation and agricultural technology, agricultural UAVs have been widely used in modern agricultural production and management. UAVs have become an inevitable choice to monitor, fertilize, and apply pesticides to plants accurately [8–10]. UAV path planning is a hot research topic at present. However, it has some problems, such as poor manual operability and high operating cost. Whether the path planning of agricultural UAVs is reasonable directly affects the success or failure of the mission. In mountainous orchards, farmland, and other complex terrain environments, UAVs often face different threat areas and obstacles, such as wind shear areas, base station towers, forest shelterbelts, agricultural facilities, and buildings [11]. Therefore, reasonable and safe flight path planning is necessary to improve obstacle avoidance performance and reduce flight costs.

Scholars in China and foreign countries have proposed various autonomous flight path planning algorithms for UAVs, which can be divided into traditional classical algorithms and swarm intelligence algorithms. Traditional classical algorithms include the Dijkstra algorithm [12], A* algorithm [13], artificial potential field method [14], and simulated annealing algorithm [15]. Vijayakumar et al. (2019) proposed an improved A* algorithm for UAV path planning to enhance the efficiency of path planning and the accuracy of determining the shortest path to some extent [16]. Xu et al. (2018) improved the artificial potential field method and applied it to UAV path planning to solve the problems of excessive randomness of search range and low convergence speed [17]. Swarm intelligence algorithms include genetic algorithm [18], particle swarm optimization (PSO) [19], Bat algorithm [20], artificial bee colony (ABC) algorithm [21], and ant colony optimization [22]. Compared with the traditional algorithm, the swarm intelligence algorithm can solve large-scale complex programming problems with nonlinearity, multipeaks, multivalleys, and nonconvexity without centralized control and a global model. Wu et al. (2018) reduced the search space by integrating constraints and search algorithm, and the global optimal UAV path planning scheme based on PSO was obtained [23]. Mozaffari et al. (2019) proposed a trajectory planning model for UAVs based on the constraints of trajectory length and trajectory angle, and the improved ABC algorithm was adopted to determine the trajectory planning scheme [24]. Wu et al. (2018) proposed an improved ABC algorithm using the K-means clustering method. The experimental results showed that the improved ABC algorithm has better convergence speed and search accuracy than the traditional ABC algorithm in solving the UAV path planning problem [25]. Mofid et al. (2018) proposed an improved UAV path planning method based on an ant colony algorithm to determine an efficient agricultural UAV path [26]. As an intelligent bionic algorithm, PSO possesses simple rules, fast convergence, and easy implementation. However, it easily falls into the dilemma of local optimization and slow convergence in the late iteration. Scholars have improved the shortcomings of PSO. Wu et al. (2017) used chaotic mapping to enhance the initial distribution of particles, and an adaptive linear acceleration coefficient was set to obtain an improved solution [27]. Singh et al. (2018) proposed nonlinear weights to optimize the PSO algorithm, and an adaptive update strategy was introduced to balance the abilities to investigate and develop complex optimization problems [28]. Lyu et al. (2016) proposed an ACMPSO algorithm based on adaptive change, and exponential inertia weight and Cauchy change step adjustment strategy were adopted to improve the convergence speed and local optimization ability of the algorithm [29]. John et al. (2017) introduced the broken-line slope inertia factor, which can flexibly adjust the slope as needed and shorten the three-dimensional trajectory length of the UAV, to solve the unsatisfactory trajectory planning problem caused by the fixed inertia factor of standard particle swarm [30]. Aiming at the problem that the algorithm optimization algorithm easily falls into a local optimum, Yang et al. (2018) used the Cauchy-Gauss mutation strategy to mutate the current optimal individual; this strategy has a good reference value for the local problem optimization [31].

In summary, studies of agricultural UAV path planning are few. UAV flight path planning can ensure the smooth completion of the flight mission and determine the optimal space flight path for the same mission. The comprehensive and rapid acquisition of information by agricultural UAVs is the premise and foundation for realizing intelligent, dynamic, and efficient management and protection of forest resources. Before a UAV performs the agricultural inspection task, it can avoid the surrounding obstacles and consume minimal operation time and energy after fully grasping the position information of the surrounding environment. Millimeter-wave radar sensors, possessing strong environmental adaptability and detection ability, can improve flight safety and reliability. On the basis of the standard PSO algorithm, the adaptive inertia weight factor and the fused Cauchy-Gaussian mutation operator are introduced to adjust the convergence speed of particles in the global–local search process. For the complex and changeable environment of the forest, sensor equipment is used to precheck the environmental targets, and a three-dimensional environment model of the UAV mission is established. Moreover, the trajectory objective function is formed by analyzing the constraints of a safe UAV flight. The simulation results demonstrate that the improved algorithm has strong robustness and adaptability in the three-dimensional environment space.

The rest of this study is organized as follows. Section 2 gives the relevant background, including a statement of the smart agriculture problem and a brief introduction to agricultural UAVs. Section 3 presents the performance constraints of agricultural UAV. Section 4 describes the algorithm design, Section 5 describes the algorithm simulation and analysis, and finally, the conclusions are summarized in Section 6.

3. Performance constraints of agricultural UAV

3.1 Performance constraints

The transportation of agricultural inspection UAVs should be considered from different aspects. On the basis of the aspects of performance constraints and mission requirements of agricultural inspection UAVs, this study established a path planning model under multiconstraint conditions. The transportation task area of the agricultural UAV was set as a space environment with length, width, and height of x, y, and z, respectively.

(1) Longest path constraint

An important factor for evaluating path planning is the length of the planned path. The shorter the planned path is, the better it is. Therefore, the transportation distance of the

logistics UAV shall not be greater than the longest path. (x_i, y_i, z_i) indicates the position of the UAV at the ith point in the three-dimensional rectangular coordinate system. The constraint is as follows:

$$d_i = \sum_{i=1}^{n} \sqrt{(x_i - x_{i-1})^2 + (y_i - y_{i-1})^2 + (z_i - z_{i-1})^2} \tag{1}$$

$$d_i \le d_{\max} \tag{2}$$

where $d_{\max}$ is the longest path of the UAV.

(2) Maximum cargo weight constraint

The weight that the logistics UAV can carry is limited, and the total weight comprises the UAV weight and cargo weight. The weight of the logistics UAV is constant. A limitation for the cargo weight exists. The upper bound constraint is:

$$M = m + n \tag{3}$$

$$n \le n_{\max} \tag{4}$$

where m is the weight of the logistics UAV, n is the weight of the goods, and $n_{\max}$ is the maximum cargo weight.

(3) Flight height constraint

The logistics UAV is affected by its performance and cargo during flight. Its flying height should be limited between the minimum and maximum flying heights. The flight height constraint is as follows:

$$h_{\min} \le h \le h_{\max} \tag{5}$$

where $h_{\min}$ is the minimum flying height, and $h_{\max}$ is the maximum flying height.

(4) Pitch angle constraint

The vertical rotation angle of the logistics UAV in the continuous flight process is limited to ensure the overall safety of logistics UAV transportation. Moreover, realizing revolutionary large-angle rotation is impossible [27]. The constraints are as follows:

$$\arctan\left[\frac{|z_i - z_{i-1}|}{\sqrt{(x_i - x_{i-1})^2 + (y_i - y_{i-1})^2}}\right] \le b \tag{6}$$

where b is the maximum pitch angle.

3.2 Threat environment model

In general, the central coordinate of a mountain in the planning area is assumed to be (x_i, y_i, z_i), and x, y, and z represent the latitude, longitude, and altitude, respectively. A planning area set is as follows:

$$\{(x_i, y_i, z_i) | 0 \ni x_i \ni x_{\max}, 0 \ni y_i \ni y_{\max}, 0 \ni z_i \ni z_{\max}\} \tag{7}$$

where $x_i \in (0, x_{\max})$ is the longitude range, $y_i \in (0, y_{\max})$ is the latitude range, and $z_i \in (0, z_{\max})$ is the altitude range.

(1) Mountain threat model

In the actual mission flight environment, the UAV must hide its body through the terrain environment. However, it collides easily with the mountain because of the maximum flying height limitation, leading to destruction [32]. In this study, mountain is defined by an exponential function, and its mathematical model is as follows:

$$z_{Momtain}(x, y) = h(i) \sum_{i=1}^{n} \exp\left[-\left(\frac{x - x_i}{x_{si}}\right)^2 - \left(\frac{y - y_i}{y_{si}}\right)^2\right] \tag{8}$$

Where $z_{Momtain}(x, y)$ is the elevation value at the point in the map, (x, y) is the mountain center coordinate at this point, (x_i, y_i) is the coordinate of the ith mountain center, x_{si} and y_{si} are the reduction rates of the ith mountain along the X axis and the Y axis, respectively, and $h(i)$ is terrain parameter.

(2) Radar threat model

Enemy detection radar is one of the main threat sources for UAVs. The closer the UAV is to the radar, the higher the probability of being detected is, and the greater the threat is to the UAV [33]. In this study, radar detection range is defined by a function expression. Its mathematical model is as follows:

$$z_{\text{Radsr}}(x, y) = K_{\text{h}}\left[R_{\max}^2 - (x - x_i)^2 - (y - y_i)^2\right] \tag{9}$$

where $z_{\text{Radsr}}(x, y)$ is the elevation value of the radar detection range, (x, y) is the radar center coordinates, (x_i, y_i) is the coordinate of the ith radar center, K_{h} is the radar detection performance coefficient, and $R_{\max}$ is the maximum radar detection range.

4. Algorithm design

4.1 Standard PSO algorithm

In the PSO algorithm, a population comprising m particles in N-dimensional space exists. The search information of particles is recorded from population iteration. In the iterative process of the algorithm, the velocity updating Formula (10) and the position updating Formula (11) are recorded as follows:

$$v_{in}^{k+1} = \omega v_{in}^{k} + c_1 r_1 (p_{in,pbest}^{k} - x_{in}^{k}) + c_2 r_2 (p_{n,gbest}^{k} - x_{in}^{k}) \tag{10}$$

$$x_{in}^{k+1} = x_{in}^{k} + v_{id}^{k+1} \tag{11}$$

where k is the number of iterations of the population search. v_{in}^{k+1} and x_{in}^{k+1} are the velocity vector and position vector of the ith particle in the nth dimension in the $k+1$ iteration, $p_{in,pbest}^{k}$ is the individual extreme value of the ith particle in the nth dimension in the nth iteration, $p_{n,gbest}^{k}$ is the global extreme value of the population in the d dimension in the kth iteration, C_1 and C_2 are the social weight and cognitive weight, respectively, ω is the inertial weight, and r_1 and r_2 are the random numbers in the interval [0,1], which can increase the randomness of search.

The value of inertia weight ω plays an important role in particle velocity. A large ω value improves the global search, weakens the ability to fall into the local extremum, and reduces the local optimization ability. In the algorithm search process, the algorithm tends to global search in the early stage, and the ω value should be large. The algorithm tends to local search in the late stage, and the ω value should be small. Therefore, ω adopts a linear change strategy. The formula is shown in (12).

$$\omega = \omega_{\max} - (\omega_{\max} - \omega_{\min})\frac{k}{k_{\max}} \tag{12}$$

where $k_{\max}$ is the maximum number of iterations of population search.

4.2 Improved standard PSO (PSO based on the Cauchy-Gaussian mutation operator)

4.2.1 Adaptive inertia weight

The search process of the algorithm is also dynamic, and the global optimal position of the search is related to the number of iterations. The weight must be set according to the distance of the global optimal position and the number of iterations to balance the relationship between search speed and search accuracy. As a result, the inertia weight can fully adapt to the change in search iterations and improve the global search ability. Therefore, this study adopted the nonlinear dynamic inertia weight coefficient method. Formula (13) is as follows:

$$\omega = \begin{cases} \omega_{\min} - \dfrac{(\omega_{\max} - \omega_{\min})(f - f_{\min})}{f_{\arg} - f_{\min}}, f \le f_{\arg} \\ \omega_{\max}, f > f_{\arg} \end{cases} \tag{13}$$

where $\omega_{\max}$ is the maximum ω value, $\omega_{\min}$ is the minimum ω value, f is the real-time target of particles, $f_{\arg}$ is the average value of particles, and $f_{\min}$ is the minimum value of particles.

4.2.2 Fusion Cauchy-Gaussian mutation operator

As an intelligent optimization algorithm, the Cauchy-Gaussian mutation operator has a low central peak value of the Cauchy mutation. Thus, it can promote global search and improve population diversity. The random number range of Gaussian distribution is relatively small. This feature has great advantages in forcing particles to jump out of the local optimum and searches near the optimal solution. The Cauchy-Gaussian operator mutates the particles in the optimal position of the current iteration. The position formula after mutation is written in (14).

$$X_{best}(k) = P_{in,pbest}(k) \times [(1 + \lambda_1 Cauchy(0,\sigma^2) + \lambda_2 Gauss(0,\sigma^2)] \tag{14}$$

where $X_{best}(k)$ is the position of the optimal individual after mutation, $P_{in,pbest}(k)$ is the position of the optimal individual in iteration, and $P_{in,pbest}(k)$ and $Gauss(0,\sigma^2)$ are the Cauchy-Gaussian mutation random number satisfying normal distribution and $Gauss(0,\sigma^2)$, respectively. λ_1 in Formula (15) and λ_2 in Formula (16) are as follows:

$$\lambda_1 = 1 - \frac{k^2}{K^2} \tag{15}$$

$$\lambda_2 = k^2 / k_{\max}^2 \tag{16}$$

where k_{max} is the maximum number of iterations in the algorithm, k represents the kth iteration, and λ_1 and λ_2 are the dynamic parameters in mutation. Influenced by the iterative process, the value of λ is usually large in the early stage of iteration to maintain the population diversity.

During the local search, the Gaussian mutation operator mutates the current optimal particle to enhance the ability to search for the optimal solution, and the particle is forced to jump out of the local extremum. It is judged according to the historical optimal fitness change rate of the particle. The particle enters the local search when the historical optimal fitness change rate is less than the threshold α for n consecutive generations. The judgment formula is as follows:

$$\left| \frac{f(P_{in}) - f(P_{in}(t-n))}{f(P_{in}(t))} \right| \le \alpha, t > n \tag{17}$$

where $f(P_{in}(t))$ is the optimal particle fitness, and α is usually set to 0.0001.

4.2.3 Optimization algorithm

The specific process of improving PSO (optimizing PSO using the Cauchy-Gaussian mutation operator) is as follows, and the algorithm flowchart is shown in Fig. 4.

Step 1: Initialize the parameters of the PSO optimized by the Cauchy-Gaussian mutation operator, including the maximum number of iterations (kmax), the number of particles (m), the position dimension (pointNum), inertia weight, social weight (c1), and cognitive weight (c2). Record the initial particle position and other parameters.

Step 2: Calculate the fitness values of particles and record the fitness values, individual extreme values, and global optimal values of all particles.

Step 3: In the iterative particle search process, carry out Cauchy variation on the optimal position of a contemporary single particle and update the particle position.

Step 4: Judge whether the particle in the current iteration is trapped in the local optimum. Enter local search and carry out Gaussian variation on the particles trapped in the local optimum; otherwise, implement Step 5.

Step 5: Update the fitness value, individual optimal value, and global optimal value of the particle. Then, update the inertia weight.

Step 6: Determine whether the iteration termination condition is met. If so, terminate the loop; if not, repeat Step 3.

5. Algorithm simulation and analysis

5.1 Simulation parameter setting

The simulation experiment was conducted in the environment of Win10 64-bit operating system, Core i7 5800H processor, and MATLAB R2014b with 16 GB RAM. In the modeling task space of 20 km × 20 km × 2000 m, the coordinates of the starting and ending points are [6,15,200] and [20,10,1000], respectively. The specific coordinate

parameters of the three-dimensional task space target are shown in Fig. 1.

The symbolic obstacles causing an unreachable target and local minimum were set on the MATLAB simulation software to verify the effectiveness of the proposed PSO algorithm based on the improved Cauchy-Gaussian mutation operator. Simulation experiments were also conducted. The simulation environment is a 20 km × 20 km × 2 km area. The path planning experiment was conducted. The experimental parameters are listed in Table 1.

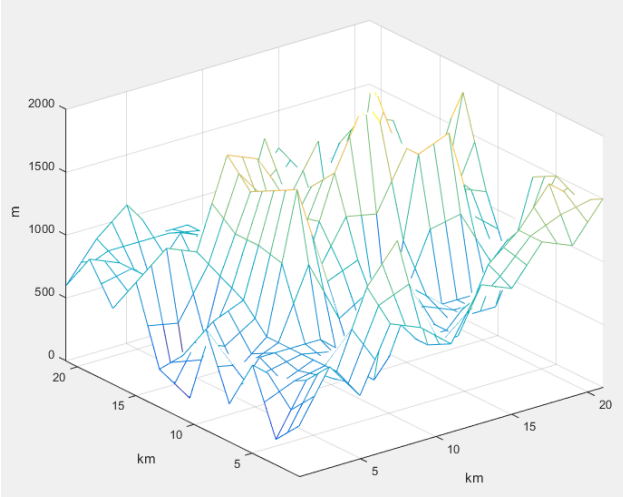

Fig. 1. Environment modeling

Table 1. Experimental parameters

Parameter	Value	Parameter	Value
Number of particles (m)	100	Maximum number of iterations (kmax)	100
Particle position dimension (pointNum)	3	Maximum inertia weight (max)	1.1
Gaussian variation	0.0001	Inertia weight	1
Particle velocity limit	0.2	Minimum inertia weight	0.4
Pause interval	0.001	Cognitive weight	2.2
Collision detection (flag)	1	Maximum social weight	1.8
Random number (r1, r2)	[0,1]	λ	[0,1]

5.2 Simulation result analysis

MATLAB 2014b was used to display the three-dimensional trajectory of the UAV through a three-dimensional coordinate system and present the three-dimensional trajectory planning path of the agricultural UAV intuitively and accurately. Under the same conditions, the proposed PSO algorithm based on the Cauchy-Gaussian mutation operator was simulated and verified in the task space environment of 20 km × 20 km × 2 km. The convergence curve of the fitness function is shown in Fig. 2, and the path planning result is presented in Fig. 3.

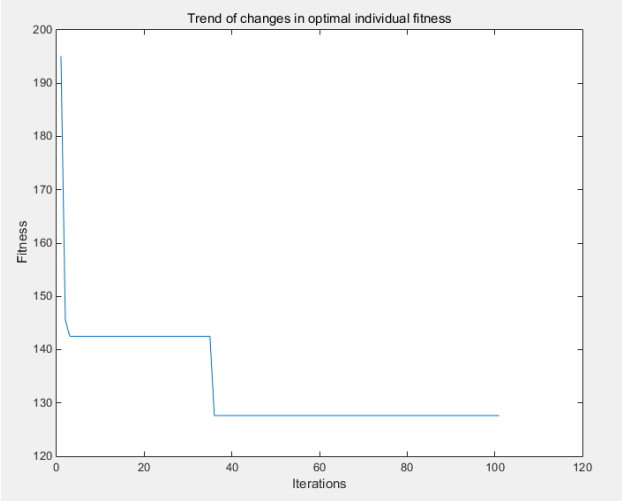

Fig. 2. Fitness function of the PSO algorithm based on the Cauchy-Gaussian mutation operator

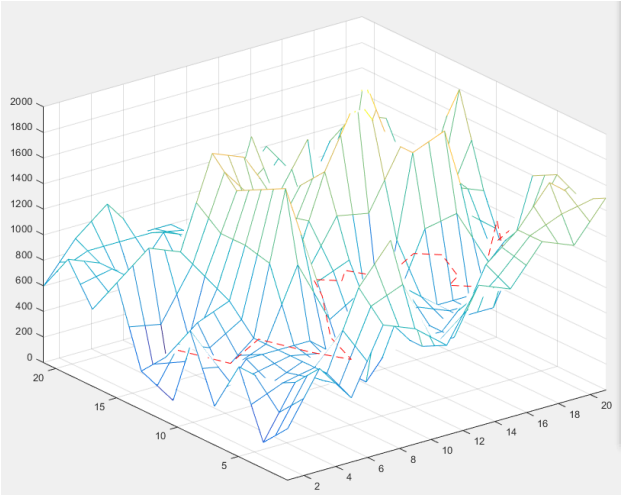

Fig.3. Path planning result of the PSO algorithm based on the Cauchy-Gaussian mutation operator

The traditional PSO algorithm was used in determining the optimal three-dimensional path of agricultural UAV in the same planning area of 20 km × 20 km × 2 km, threat model position, starting point, and target point coordinate position to verify the effectiveness of the proposed PSO algorithm optimized by the Cauchy-Gaussian mutation operator. The convergence curve of the fitness function of the traditional PSO algorithm is shown in Fig. 4, and the path planning result is shown in Fig. 5. In Fig. 5, the red dotted line is the UAV path planning curve of the PSO algorithm optimized by the Cauchy-Gaussian mutation operator, and the blue dotted line is the UAV path planning curve of the traditional PSO algorithm.

The traditional PSO algorithm was used in determining the optimal three-dimensional path of agricultural UAV in the same planning area of 20 km × 20 km × 2 km, threat model position, starting point, and target point coordinate

position to verify the effectiveness of the proposed PSO algorithm optimized by the Cauchy-Gaussian mutation operator. The convergence curve of the fitness function of the traditional PSO algorithm is shown in Fig. 4, and the path planning result is shown in Fig. 5. In Fig. 5, the red dotted line is the UAV path planning curve of the PSO algorithm optimized by the Cauchy-Gaussian mutation operator, and the blue dotted line is the UAV path planning curve of the traditional PSO algorithm.

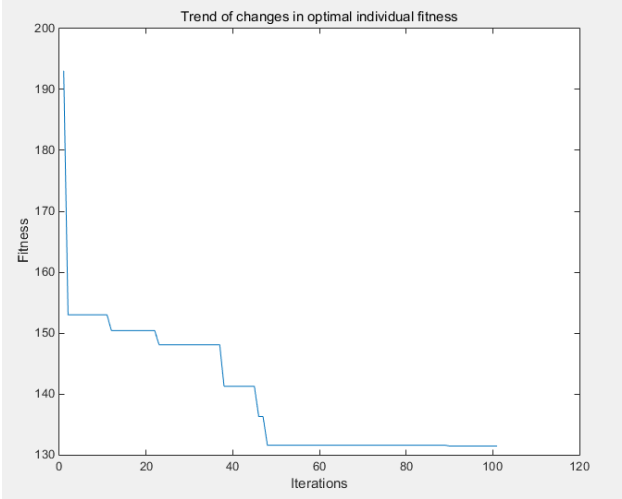

Fig. 4. Fitness function of the PSO algorithm

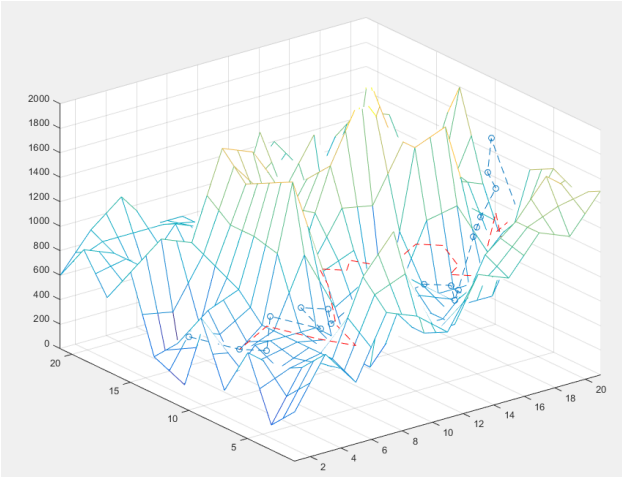

Fig. 5. Comparison of the path planning results of the PSO algorithm optimized by the Cauchy-Gaussian mutation operator and the traditional PSO algorithm

The analysis of Fig. 5 indicates that flight path planning algorithms can form smooth curved paths during the flight from the starting point to the terminal point. In the flight path results of the PSO algorithm, the obstacle avoidance distance is relatively long, and the flight path curve fluctuates greatly. Overall, the flight path effect of the PSO algorithm is good, but the local optimization is imperfect. The PSO algorithm optimized by the improved Cauchy-Gaussian mutation operator has better overall local effects than the PSO algorithm. As shown in Figs. 2 and 4, the number of iterations of the PSO algorithm is approximately 45 times, which is stable near the optimal fitness value. The number of iterations of the PSO algorithm optimized by the improved Cauchy-Gaussian mutation operator is approximately 38 times, and the optimal fitness value is stable.

The PSO algorithm optimized by the Cauchy-Gaussian mutation operator is superior to the PSO algorithm in the process of fast convergence and reaching the optimal fitness value. The comparison of Figs. 3 and 5 show that the proposed PSO algorithm optimized by the Cauchy-Gaussian mutation operator has a smooth curve curvature change, small fluctuation amplitude, and low flight path consumption cost. With a low threshold of fitness function and a high iterative convergence speed, the proposed PSO algorithm can find the optimal value faster than other algorithms. The comparison results of convergence time and UAV track length between the proposed PSO algorithm and the traditional PSO algorithm are shown in Table 2.

Table. 2. Comparison results of the two algorithmsAlgorithm

	Convergence time (s)	**Path length (km)**	**Fitness function**
PSO algorithm optimized by the Cauchy-Gaussian mutation operator	36.726	42.327	129.112
Traditional PSO algorithm	40.368	48.470	130.874

Table 2 shows that the convergence time of the PSO algorithm optimized by the Cauchy-Gaussian mutation operator is 3.46 s shorter than that of the traditional PSO algorithm, indicating a decrease of 9.021%. The path length is 6.173 km shorter than that of the traditional PSO algorithm, indicating a decrease of 12.6735% in the same experimental environment. The simulation results show that the PSO algorithm optimized by the Cauchy-Gaussian mutation operator not only effectively improves the search speed of agricultural UAV path planning but also shortens the path length. Moreover, the path searching efficiency and algorithm optimization of the proposed PSO algorithm optimized by the Cauchy-Gaussian mutation operator are superior to those of the traditional PSO. The comparison of the experimental results shows that the proposed PSO algorithm can effectively avoid threats and plan the optimal flight path in the three-dimensional path planning of UAVs. This process can successfully decrease search time and path length, thereby verifying the effectiveness and progress of the proposed PSO algorithm optimized by the Cauchy-Gaussian mutation operator.

6. Conclusions

The defects of the traditional PSO algorithm were analyzed, and the corresponding solution was proposed to improve the three-dimensional path planning of the logistics UAV. The traditional PSO algorithm was improved, and the Cauchy-Gaussian mutation operator was used to solve the unreachable problem. When the UAV was in the local extremum, the Cauchy-Gaussian mutation operator strategy was taken to construct the virtual target point and solve the local minimum problem under the combined action of obstacle repulsion, target point gravity, and virtual target point gravity. The simulation results show that the optimal flight path can be effectively planned by optimizing the Cauchy-Gaussian mutation operator and improving the

traditional PSO algorithm. Thus, agricultural UAVs can avoid all obstacles and safely reach the target point.

This study investigated the application of the PSO algorithm optimized by the Cauchy-Gaussian mutation operator in the path planning of agricultural UAVs. The millimeter-wave radar was used to predetect the environment. Thus, UAVs can perceive and adapt to the environment in advance, thereby enhancing the positioning accuracy of environmental targets and improving flight safety. The simulation results show that compared with the convergence value of the traditional PSO algorithm, the fitness standard difference of the proposed PSO algorithm is reduced by 1.346%. Thus, the proposed PSO algorithm has better robustness and higher convergence accuracy than the traditional PSO algorithm in the path planning process. Compared with the traditional PSO algorithm, the proposed PSO algorithm improves the time cost by 9.21% and enhances the timeliness of UAV operation. The results show that the proposed path planning method helps ensure the stability and safety of UAV trajectory planning. Given that the dynamic target of the agricultural UAV changes in the working environment, no dynamic target exists in the study environment. In future work, the obstacles of UAVs in dynamic environments will be further studied.

References

[1] H. Y. Zhang, Y. B. Lan, and S. Wen, "Research progress in rotor airflow model of plant protection UAV and droplet motion mechanism," *Trans. ASAE.*, vol. 36, no. 22, pp. 1-12, Nov. 2020.

[2] F. H. Yu, Y. L. Cao, and T. Y. Xu, "Precision fertilization by UAV for rice at tillering stage in cold region based on hyperspectral remote sensing prescription map," *Trans. ASAE.*, vol. 36, no. 15, pp. 103-110, Aug. 2020.

[3] Y. Y. Liu, Y. Ru, and C. Qing, "Design and test of real-time monitoring system for UAV variable spray," *Trans. Chin. Soc. Agric. Mach.*, vol. 51, no. 7, pp. 91-99, Jul. 2020.

[4] H. C. Zhao, H. Q. Zhou, and S. H. Wang, "Quantum PSO algorithm of three-dimensional path planning of unmanned aerial vehicle," *Aerosp. Control*, vol. 39, no. 1, pp. 40-45, Jan. 2021.

[5] F. L. L. Medeiros and J. D. S. Da. Silva, "Dijkstra algorithm for fixed-wing UAV motion planning based on terrain elevation," *in Proc. 2010-20th Bra. Sympo. On. AI*, *Theory*, Sao Paulo, SP, BR, 2010, pp. 213-222.

[6] A. Krizhevsky, I. Sutskever, and G. E. Hinton, "ImageNet classification with deep convolutional neural networks," *Commun. ACM.*, vol. 60, no. 6, pp. 84-90, Jun. 2017.

[7] D. Silver, A. Huang, and C. J. Maddison, "Mastering the game of go with deep neural networks and tree search," *Nature*, vol. 529, no. 7587, pp. 484-489, Jan. 2016.

[8] J. Sun, J. Tang, and S. Lao, "Collision avoidance for cooperative UAVs with optimized artificial potential field algorithm," *IEEE Access*, vol. 5, pp. 18382-18390, Aug. 2017.

[9] D. Silver, J. Schrittwieser, and K. Simonyan, "Mastering the game of Go without human knowledge," *Nature*, vol. 550, no. 7676, pp. 354-359, Oct. 2017.

[10] R. Marie, H. B. Said, J. Stéphant, and O. Labbani-Igbida, "Visual servoing on the generalized Voronoi diagram using an omnidirectional camera," *J. Intell. Robot. Syst.*, vol. 94, no. 3-4, pp. 793–804, Jun. 2019.

[11] O. Vinyals, I. Babuschkin, and W. Czarnecki, "Grandmaster level in StarCraft II using multi-agent reinforcement learning," *Nature*, vol. 1, pp. 1-5, Nov. 2019.

[12] J. Hwangbo, J. Lee, and A. Dosovitskiy, "Learning agile and dynamic motor skills for legged robots," *Sci. Robot.*, vol. 4, pp. 1-13, Jan. 2019.

[13] T. C. Barkdoll, D. P. Gaver, K. D. Glazebrook, P. A. Jacobs, and S. Posadas, "Suppression of enemy air defenses (SEAD) as an information duel," *Nav. Res. Log.*, vol. 49, no. 8, pp. 723-742, Mar. 2002.

[14] M. Haque, M. Egerstedt, and A. Rahmani, "Multilevel coalition formation strategy for suppression of enemy air defenses missions," *J Aerosp. Inform. Syst.*, vol. 10, no. 6, pp. 287-296, Jun. 2013.

[15] V. Mnih, K. Kavukcuoglu, D. Silver et al., "Human-level control through deep reinforcement learning," *Nature*, vol. 518, no. 7540, pp. 529-533, Feb. 2015.

[16] D. M. Vijayakumari, S. Kim, J. Suk, and H. Mo, "Receding-horizon trajectory planning for multiple UAVs using PSO," *in Proc. AIAA Scitech 2019 Forum*, *Theory*, Daejeon, KR, 2019, pp. 1165-2019.

[17] Y. Xu, L. Xiao, D. Yang, Q. Wu, and L. Cuthbert, "Throughput maximization in multi-UAV enabled communication systems with difference consideration," *IEEE Access*, vol. 6, pp. 55291-55301, Jun. 2018.

[18] A. Al-Hourani, S. S. Kandeepan, and S. Lardner, "Optimal LAP altitude for maximum coverage," *IEEE. Wirel. Commun. Le.*, vol. 3, no. 6, pp. 569-572, Dec. 2014.

[19] M. Mozaffari, M. W. Saad, M. Debbah, and D. Mérouane, "Unmanned aerial vehicle with underlaid device-to-device communications: performance and tradeoffs," *IEEE. Wirel. Commun. Le.*, vol. 15, no. 6, pp. 3949-3963, Jun. 2016.

[20] M. Mozaffari, M. W. Saad, M. Debbah, and M. Debbah, "Efficient deployment of multiple unmanned aerial vehicles for optimal wireless coverage," *IEEE. Commun. Lett.*, vol. 20, no. 8, pp. 1647-1650, Aug. 2016.

[21] F. Wu, D. Yang, L. Xiao, and L. Cuthbert, "Energy consumption and completion time tradeoff in rotary-wing UAV enabled WPCN," *IEEE Access*, vol. 7, pp. 79617-79635, Jul. 2019.

[22] Y. Zeng and R. Zhang, "Energy-efficient UAV communication with trajectory optimization," *IEEE. Wirel. Commun. Le.*, vol. 16, no. 6, pp. 3747-3760, Jun. 2017.

[23] Q. Wu, Y. Zeng, and R. Zhang, "Joint trajectory and communication design for multi-UAV enabled wireless networks," *IEEE. Wirel. Commun. Le.*, vol. 17, no. 3, pp. 2109-2121, Mar. 2018.

[24] M. Mozaffari, W. Saad, M. Bennis, and M. Debbah, "Mobile unmanned aerial vehicles UAVs for energy-efficient internet of things communications," *IEEE. Wirel. Commun. Le.*, vol. 16, no. 11, pp. 7574-7589, Nov. 2017.

[25] Q. Wu and R. Zhang, "Common throughput maximization in UAV-enabled multiuser OFDMA systems with delay consideration," *IEEE. Wirel. Commun. Le.*, vol. 66, no. 12, pp. 6614-6627, Jan. 2018.

[26] O. Mofid and S. Mobayen, "Adaptive sliding mode control for finite-time stability of quad-rotor UAVs with parametric uncertainties," *ISA. T.*, vol. 72, pp. 1-14, Jan. 2018.

[27] Q. Wu, W. Li, D. W. K. Chen, D. W. K. Ng, and R. Schober, "An overview of sustainable green 5G networks," *IEEE Wirel. Commun.*, vol. 24, no. 4, pp. 72-80, Apr. 2017.

[28] A. K. Singh and L. Dewan, "Adaptive-PID with sliding mode control for longitudinal flight of an UAV," *Int. J. Eng. Tech.*, vol. 4, pp. 1-6, Apr. 2018.

[29] J. Lyu, R. Y. Zeng, and R. Zhang, "Cyclical multiple access in UAV-aided communications: a throughput-delay tradeoff," *IEEE Wirel. Commun. Le.*, vol. 5, no. 6, pp. 600-603, Dec. 2016.

[30] A. A. B. John and R. Dutta, "Cooperative trajectory planning in an intercommunicating group of UAVs for convex plume wrapping," *in Proc. 38th Sarnoff Symposium*, *Theory*, Newark, MA, 2017, pp. 7-12.

[31] D. Yang, Q. Wu, and Y. Zeng, "Energy trade-off in ground-to-UAV communication via trajectory design," *IEEE T. Veh. Technol.*, vol. 67, no. 7, pp. 6721-6726, Sep. 2018.

[32] H. Zhang, R. Yang, and J. Wu, "Research on multi-aircraft cooperative suppressing jamming embattling in electronic warfare planning," *J. Syst. Eng. Electron.,* vol. 39, pp. 542-548, Mar. 2017.

[33] H. He, S. Zhang, Y. Zeng, and R. Zhang, "Joint altitude and beamwidth optimization for UAV-enabled multiuser communications," *IEEE Commun. Lett.*, vol. 22, no. 2, pp. 344-347, Feb. 2018.